Available online at www.ewijst.org

ISSN: 0975-7112 (Print)
ISSN: 0975-7120 (Online)

Environ. We Int. J. Sci. Tech. 13 (2018) 29-45

Environment & We
An International
Journal of Science
& Technology

Estimation of Temporal Land Surface Temperature using Thermal Remote Sensing of Landsat-8 (OLI) and Landsat-7 (ETM+): A study in Sainj River Basin, Himachal Pradesh, India

Pawan Kumar Thakur and Vaibhav E. Gosavi*
G. B. Pant National Institute of Himalayan Environment and Sustainable Development, Himachal Regional Centre, Mohal-Kullu, 175 126 (H.P.) India.
*Email: *vaibhavgosavi8@gmail.com*

Article history:
Received 28 February 2018
Received in revised form
16 March 2018
Accepted 31 March 2018
Available online
31 March 2018

Keywords:
Land Surface Temperature;
IHR;
Thermal Remote Sensing;
Split-Window;
NDVI;
Land use/land cover;
MODIS

Abstract

Land Surface Temperature (LST) has an essential role in studies related to hydrological cycle, climate change, land use/land cover change, soil moisture and vegetation water stress. The estimation of LST plays important role in numerical modeling especially in physical based hydrological models where water balance/budgeting of the catchment is an important component. Application of Thermal Remote Sensing technique provides opportunity to retrieve LST of different land cover at local scale, which was very cumbersome and uneconomic in conventional way. Present study was conducted in downstream part of Sainj river basin in Himachal Pradesh of Indian Himalayan Region (IHR), wherein we examine the change in LST over different land use/land cover of the area over the period of time where developmental activities alters the natural ecosystem in relation to water and land use. LST was derived using Landsat-7 Enhanced Thematic Mapper Plus (ETM+) for October 2001 using Single-Window algorithmand Landsat-8 OLI (Operational Land Imager) for October 2016 using Split-Window (SW) algorithm. NDVI threshold was used for estimating land surface emissivity. The spatial distribution of LST ofLandsat-7 of 18th October 2001 ranged from minimum 6.15°C to maximum 36.10°C with a mean of 19.98°C and standard deviation of 6.09;whereas, for Landsat-8 (OLI), of 22nd October 2016 ranged from minimum 7.16°C to maximum 33.31°C with a mean of 19.62 °C and standard deviation of 4.95. For validation, the standard daily LST product of MODIS has been used for both algorithms. Further the corresponding land use/land cover change was also analyzed to understand the effect of land use changes on the behavior of land surface temperature

Introduction

Land Surface Temperature (LST), a key geophysical parameter, has an essential role in studies related to hydrological cycle, climate change, land use/land cover change, soil moisture, vegetation water stress etc. LST is the skin temperature of the ground; where for bare soil surface it is soil surface temperature; for dense vegetation it is canopy surface temperature; and for sparse vegetated ground LST is determined by the temperature of the vegetation canopy, vegetation body and the soil surface (Qin and Kanieli 1999). It is governing parameter that control water and energy nexus between land and atmosphere (Yu et al. 2014). The estimation of LST pays important role in numerical modeling especially in physical based hydrological models where water balance/budgeting of the catchment is an important component. LST varies with the complexity of the land cover that changes naturally as well as due to anthropogenic activities. In studies, related land surface modeling, climate change studies, impacts of urbanization, drought monitoring and/or assessment and irrigation project, LST has significance application while dealing with energy balance and ET on regional basis (Kustas and Anderson 1996; Ramanathan et al. 2001; Kalnay and Cai 2003; Wan et al. 2004; Karnieli et al. 2010; Nikam et al. 2016;). The knowledge of LST is necessary for many environmental studies and management activities of Earth's surface resources (Li and Becker 1993). Due to dynamic nature of LST, both spatially and temporally, the conventional LST measurement techniques are cumbersome, uneconomic and insufficient for user (Nikam et al. 2016). Remote sensing can provide information on surface albedo, vegetation index, surface emissivity and surface temperature, which used as inputs for surface heat flux studies, are otherwise difficult in obtaining the spatial and temporal information from traditional ground based in situ measurement (Chakraborty et al. 2013; Singh, 2016; Kanga et al., 2017). Retrieval of LST using thermal infrared bands of satellite images is the most effective way to derive energy balance and ET on regional basis (Parida et al. 2008). The Synoptic and repeated coverage of land surface by remote sensing satellites provides good opportunity to retrieve LST, at local to global scale from fortnightly to sub-daily temporal resolution (Rozenstein et al. 2014).

Landsat satellite series provides the data for retrieval of LST for longer period of time. Whereas, data also available from Moderate Resolution Imaging Spectroradiometer (MODIS) products from which one can retrieve LST for various purposes. Thematic Mapper (TM) onboard Landsat 5 and Enhanced Thematic Mapper Plus (ETM+) onboard Landsat 7 and Landsat 8 (OLI) provided thermal data using just one LWIR band with higher spatial resolution with a 16-day temporal resolution (Nikam et al. 2016). However, parameter like LST can only be retrieved through complex atmospheric transmittance/radiance codes (Li et al. 2013b). Among them, researchers used Single channel/window algorithm, Split-Window (SW) algorithm and Radiative Transfer Theory (RTT) to retrieve the LST from satellite data products.

Owing to the importance of LST in various scientific fields as mentioned earlier, LST acts as a governing parameter in water and energy exchange between land and atmosphere. Therefore, its application in studying impacts of change in land use/land cover on surface temperature is of great importance in context of climate change and in the era of development. Keeping in view the importance of the LST and available data products/platforms for retrieving the LST, present study was conducted in downstream part of Sainj river basin, Kullu district, in Himachal Pradesh of Indian Himalayan Region (IHR), wherein we examine the change in LST over different land use/land cover in the catchment area over the period of time where developmental activities alters the natural ecosystem in relation to water and land use. LST was derived using Landsat-7 Enhanced Thematic Mapper Plus (ETM+) for October 2001 using Single-Window algorithm and Landsat-8 OLI (Operational Land Imager) for October 2016 using Split-Window (SW) algorithm. Further, to validate the estimated LST, the standard daily LST product of MODIS has been used for both the algorithm.

Materials and Methods

Study area

The study area falls in the downstream part of the Sainj river basin, a tributary of Beas river in Kullu district of Himachal Pradesh. The study area (81 km^2) located between latitudes 31°43′3″ and 31°48′51″N and longitudes 77°13′28″ and 77°20′13″E and falls under the left bank of Upper Beas river system (Fig. 1). A greater part of the Sainj river sub-basin lying in the Lesser Himalaya is hilly with deep and narrow valleys (V and U shaped) separated by spurs and ridges. The altitude of the tract varies from 978 m at the mouth and highest hilly point at 3200 m above mean sea level. The climate is typically the Western Himalayan temperate and alpine type. Sainj river basin receives an average annual rainfall of 1000 mm and more than 50% of which is received during the south-west monsoon (June-Sept). Snowfall (345 mm average annual) in the region confined to upper reaches of the basin during winter season only. At Larji (the outlet of the study area watershed), the mean monthly temperature ranged from minimum 8.7^0C in January to the maximum of 26.3^0C during June (Singh et al.2008). The catchment area villages engaged in rain fed farming and experiencing water shortage for domestic as well as agricultural use along the slope of the river valley in dry season.

Data used and methodology

Cloud Free Landsat 7 (ETM+) and Landsat 8 (OLI) satellite data in the years of October, 2001 and 2016 for the study area has been downloaded from USGS Earth Explorer website. MODIS datasets of same period were downloaded from MODIS data product website. All the datasets were pre-processed and projected to the Universal Transverse Mercator (UTM) projection system. The details of the satellite data collected are shown in Table 1.

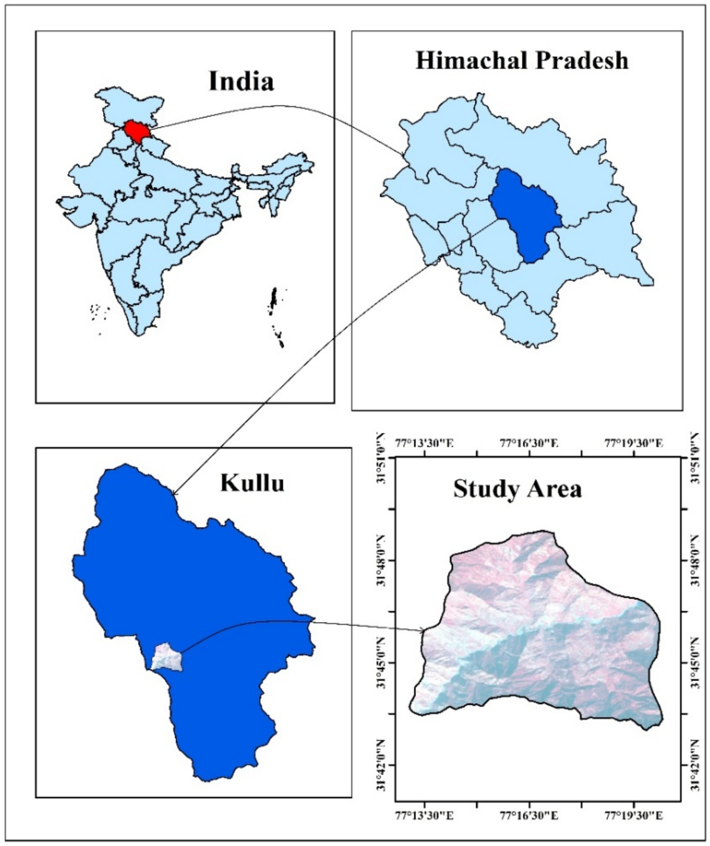

Fig. 1 Location map of the study area

Table 1 General information of Landsat 8 (OLI), Landsat 7 (ETM+) and MODIS datasets

Sensor / Satellite	**No. of Bands**	**Resolution (m/Km)**	**Path/ Row & Reference system**	**Date of Acquisition**
OLI	9	30 m	WRS-II/146/40	19-10-2016
TIR	2	100 m	WRS-II/146/40	19-10-2016
ETM+	7	30	WRS-II/146/40	18-10-2001
TIR	2	30	WRS-II/146/40	18-10-2001
MODIS (TIR)	2	1 Km	WRS-II/146/40	18-10-2001
MODIS (TIR)	2	1 Km	WRS-II/146/40	19-10-2016

In the present study, land use/land cover map was prepared using Landsat 7 and 8 satellite images. For estimation of LST, two algorithms namely, Single Window/Single Channel and Split Window have been used from Landsat 7 (ETM+) and Landsat 8 (OLI) satellite data. Finally, the retrieved LST from both techniques/algorithms were validated using MODIS datasets.

Land use/Land cover

Using bands 2, 3, 4, 5 and 7 of the pre-processed images of Landsat 7 & 8, the land use/cover pattern was mapped by Supervised Classification with the SVM (Support Vector Machine) classification algorithm of Envi (Environmental Visualization Imagine) 5.1 and ERDAS 2015 (Earth Resource Data Analysis System) software. ArcGIS 10.3.1 software was also used for spatial analysis and generating thematic layers. Supervised Classification had been used for the built-up change detection especially in the land use /cover over the period of (2001 to 2016) time. In the ERDAS 2015 for better classification result, some indices such as Normalized Difference Vegetation Index (NDVI), and Normalized Difference Built up Index (NDBI) were also applied to classify the Landsat 7 (ETM+) images at a spatial resolution with 30 m of 2001 and Landsat 8 (OLI) 2016, at a spatial resolution 30 m.

Split Window Algorithm for LST estimation from Landsat-8 data of October 2016

LST was calculated by applying a structured mathematical algorithm of Split-Window (SW) algorithm. The operational algorithm of Split-window (SW) was first proposed by McMillin (1975) who retrieve sea surface temperature (SST) using difference in atmospheric absorption of two adjacent LWIR bands. Price (1984) implemented SW algorithm for measurement of LST using AVHRR data from NOAA 7. Thereafter, researchers have implemented and modified the SW algorithm for different purposes. For present study, we used the simplified formulation of SW algorithm by Jimenez-Munoz and Sobrino (2008) as follows:

$$T_S = TB_{10} + C_1 \times (TB_{10}-TB_{11}) + C_2 \times (TB_{10}-TB_{11})^2 + C_0 + (C_3+C_4+w) \times (1-\varepsilon) + (C_5+C_6+w) \times \Delta\varepsilon \quad (1)$$

where; Ts is land surface temperature (^oK); TB_{10} and TB_{11} are brightness temperature of band 10 and 11 of Landsat 8 (^oK) respectively; ε is mean land surface emissivity ($0.5 \times [\varepsilon_{10}+\varepsilon_{11}]$) of TIR bands; w is atmosphericwater vapor content (g/cm^2); Δ ε represent the difference in land surface emissivity (ε_{10} - ε_{11}) and C_0 – C_6 are split-window coefficients. Split window coefficients values were given by Skokovic et al. (2014) for TIRS of Landsat 8, available in public domain and same has been used here (Table 2). Therefore, very simple but yet robust SW algorithm was selected to retrieve LST using Landsat 8 TIRS data.

Derivation of NDVI Image

The Normalized Difference Vegetation Index (NDVI) is a measure of the amount and vigor of vegetation at the surface. The reason NDVI is related to vegetation is that healthy vegetation reflects very well in the near infrared part of the spectrum. The value is then normalized to -1<=NDVI<=1 to partially account for differences in illumination and surface slope. The index is defined by Eq. 2. The basic algorithm of a spectral index takes the form of a ratio between two spectral bands Red and near infrared (NIR). This index is calculated by subtracting Red band from NIR band, and dividing by the sum of Red band from NIR band. Estimation of Normalized Difference Vegetation Index (NDVI) using Landsat 8 (OLI) sensor and Landsat 7 (ETM+) data after layer stacking of Band 2,3,4,5 and 7 using algorithm shown in Eq. 2

$$\text{NDVI} = \frac{\text{BAND 4} - \text{BAND 3}}{\text{BAND 4} + \text{BAND 3}} \qquad (2)$$

Table 2 Split Window coefficient values for TIRS of Landsat 8

Constants	Value
C0	-0.268
C1	1.378
C2	0.183
C3	54.300
C4	-2.238
C5	-129.200
C6	16.400

Single Window/ Channel Algorithm for LST estimation from Landsat-7 data of October 2001

The digital number (DN) of thermal infrared band is converted in to spectral radiance (Lλ) using the equation supplied by the Landsat user's hand book. We estimate Top of Atmospheric Spectral Radiance of TIRS Band 6 and Landsat ETM+ sensor of Band 2-5 individually using the algorithm given below. This algorithm transform raw image into spectral radiance image. Using ERDAS IMAGINE 2015 model maker we implement algorithm of Eq. 3 to perform the task.

$$L\lambda = \frac{\text{LMAX} - \text{LMIN} * \text{DN} - 1 + \text{LMIN}}{\text{QCALMAX} - \text{QCALMIN}} \qquad (3)$$

where;

LMAX - the spectral radiance that is scaled to QCALMAX in W/(m2 * sr * µm)
LMIN - the spectral radiance that is scaled to QCALMIN in W/(m2 * sr * µm)
QCALMAX - the maximum quantized calibrated pixel value (corresponding to LMAX) in DN = 255
QCALMIN - the minimum quantized calibrated pixel value (corresponding to LMIN) in DN = 1
LMAX and LMIN are obtained from the Meta data file available with the image and are given in the Table 3 and 4.

Table 3 Landsat-8 (OLI) Sensor thermal band and calibration constant values of Lλ

Band no	Satellite/ Sensor	LMAX	LMIN
10	Landsat8 /OLI High gain	22.00180	0.10033
10	Landsat8/ OLI Low gain	22.00180	0.10033
11	Landsat8/ OLI High gain	22.00180	0.10033
11	Landsat8/ OLI Low gain	22.00180	0.10033

Table 4 Landsat-7 (ETM+) Sensor thermal band and calibration constant values of Lλ

Band no	Satellite/ Sensor	LMAX	LMIN
6.1	Landsat7 /ETM+ High gain	12.65	3.200
6.2	Landsat7 /ETM+ Low gain	17.04	0.000

The effective at-sensor brightness temperature (TB) which is the microwave radiation radiance traveling upward from the top of Earth's atmosphere was obtained from the spectral radiance using Plank's inverse function. The calibration process has been done for converting thermal DN values of thermal bands of TIR to Brightness Temperature (TB). To calculate TB (in Kelvin) of an area, we required the Top of Atmospheric (TOA) spectral radiance of (Lλ). TB for both the TIRs bands was calculated by Eq. 4.

$$T_B = \frac{K2}{\text{In}\,(1+\frac{K1}{L\lambda})} \qquad (4)$$

where, K_1 and K_2 are thermal conversion constants for each TIRS bands for Landsat 8 and Landsat 7 and values of these constants are given in Table 5 and 6.

Table 5 K_1 and K_2 values for Landsat 8 TIRS bands

Thermal Constant	Band 10	Band11
K_1	1321.08	1201.14
K_2	777.89	480.89

Table 6 K_1 and K_2 value for Landsat 7 ETM+ TIRS bands

Sensor	K_1	K_2
Landsat7 /ETM+	666.09	1282.71

Brightness Temperature is the electromagnetic radiation traveling upward from the top of the Earth's atmosphere. Thermal calibration process done by converting thermal DN values of raw thermal bands of TIR sensor using ERDAS IMAGINE 2015 model maker. The final Land Surface Temperature (LST) in Kelvin is estimated by the following Eq. 5.

$$LST = \frac{T\,B}{1+(\lambda\,TB/p)*\text{Ine}} \qquad (5)$$

where;

Lλ - the wavelength of the emitted radiance which is equal to 11.5μm.
ρ - h.c/σ,
σ - Stefan Boltzmann's constant which is equal to 5.67 x 10^{-8} Wm^{-2} K^{-4},
h - Plank's constant (6.626 x 10^{-34} J Sec),
c - velocity of light (2.998 x 108 m/sec) and
ε - the spectral emissivity.
In this present study spectral emissivity coefficient is taken as unity. For all the calculations at pixel level of the image, models were developed using spatial model maker of ERDAS Imagine 2015.

Validation of retrieved LST

Validation is required for independent assessment of accuracy and uncertainty of the derived output (Nikam et al. 2016). As LST is estimated from thermal remote sensing datasets by using complex processes and inherent assumptions regarding atmospheric parameters; therefore, it is necessary to evaluate its accuracy which is helpful for both users and developers. (Li et al. 2013a). To validate the retrieved LST values, standard LST products of same area and same time period can be used. But due to dynamic nature of LST, both spatially and temporally, it is impossible to get ground based values to cross-validate the retrieved LST. The same hurdle was faced in present study. Therefore, due to non-availability of ground observed LST data, the cross-validation approach has been used for validation of retrieved LST; wherein, we used standard datasets of MODIS LST products which having accuracy within the range of 1^{o}K (Wan et al. 2004) to validate the LST retrieved for Landsat 7 and 8. The MODIS datasets were downloaded from MODIS products website https://lpdaac.usgs.gov/dataset_discovery/modis/modis_products_table/mod11a1). Standard procedure was followed for converting the LST data from sinusoidal projection system to UTM projection system and to generate MODIS LST values for the study area.

Results and Discussion

Present study has been undertaken to analyze the potential of multispectral satellite data using spectral classification and to retrieve LST parameter. Different temporal satellite datasets of Landsat-7 (ETM+) from 18th October 2001 and Landsat-8 (OLI) of 19th October 2016 were taken for the purpose. We studied the change in land use/land cover of the study area for two period: 2001 and 2016 corresponding to LST product datasets to examine the change in LST over the study area.

Six land use/land cover categories are identified in the study area viz., (i) water bodies (ii) built up/settlements (iii) forest/dense area (iv) agriculture/plantation area (v) vegetation/scrub area and (vi) bare/open land. It has been observed that there is increase in the built-up area from 2001 to 2016 and the physical expansion of the area has increased from 7.73 km^2 representing about 9.47% of the total area in 2001 to 9.46 km^2

(11.65%) in 2016. Thus, a net expansion of 1.73 km^2 is noticed over the time period of 16 years. This change in built-up area attributed to human settlement and developmental project such as hydropower projects and other schemes. Further, there is decrease in forested area and increase in vegetation and barren land. This may be attributed to change in land use for the orchard development, encroachment in the forested area and disturbed project sites because of the developmental projects in study area. The consolidated status of land use/land cover for the year 2001 and 2016 is given in Table 7 and same has been shown in Fig. 2 and 3.

Table 7 Status of Land Use/Land Cover in the study area

LU/LC Categories	October, 2001		October, 2016	
	Area in km^2	Percent (%)	Area in km^2	Percent (%)
Water Bodies	1.05	1.29	0.98	1.22
Built up/Settlements	7.73	9.47	9.46	11.65
Forest/Dense area	41.82	51.25	32.23	39.65
Agriculture/Plantation	19.1	23.40	15.75	19.38
Vegetation/scrub area	5.83	7.15	12.66	15.58
Barren/open Land	6.06	7.43	10.17	12.52

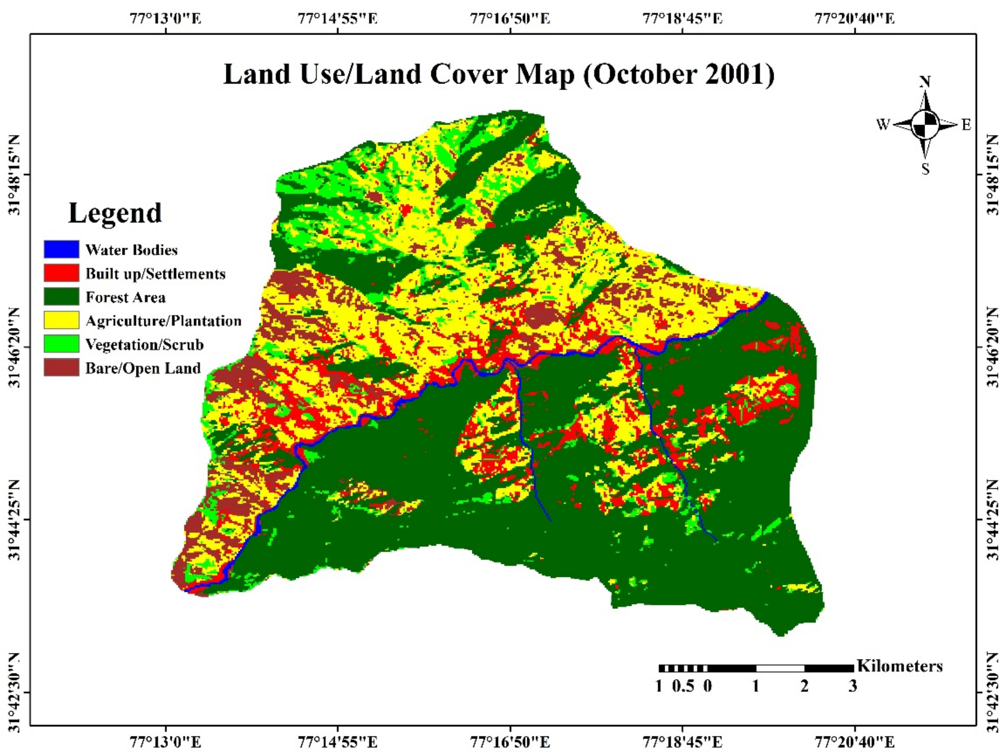

Fig. 2 Land use/land cover of the study area (Year 2001)

The NDVI values for study area were calculated for the year 2001 and 2016 using Landsat 7 and Landsat 8 satellite images respectively. The value for NDVI for the year

2001 ranges from - 0.18 (low) to 0.57 (high); the forested area have high values of NDVI followed by agricultural land (Fig. 2 and 4). For the year 2016, NDVI value ranges from - 0.09 (low) to 0.48 (high). This clearly shows the healthy vegetative condition in year 2001 as compare to 2016 (Fig. 3 and 5).

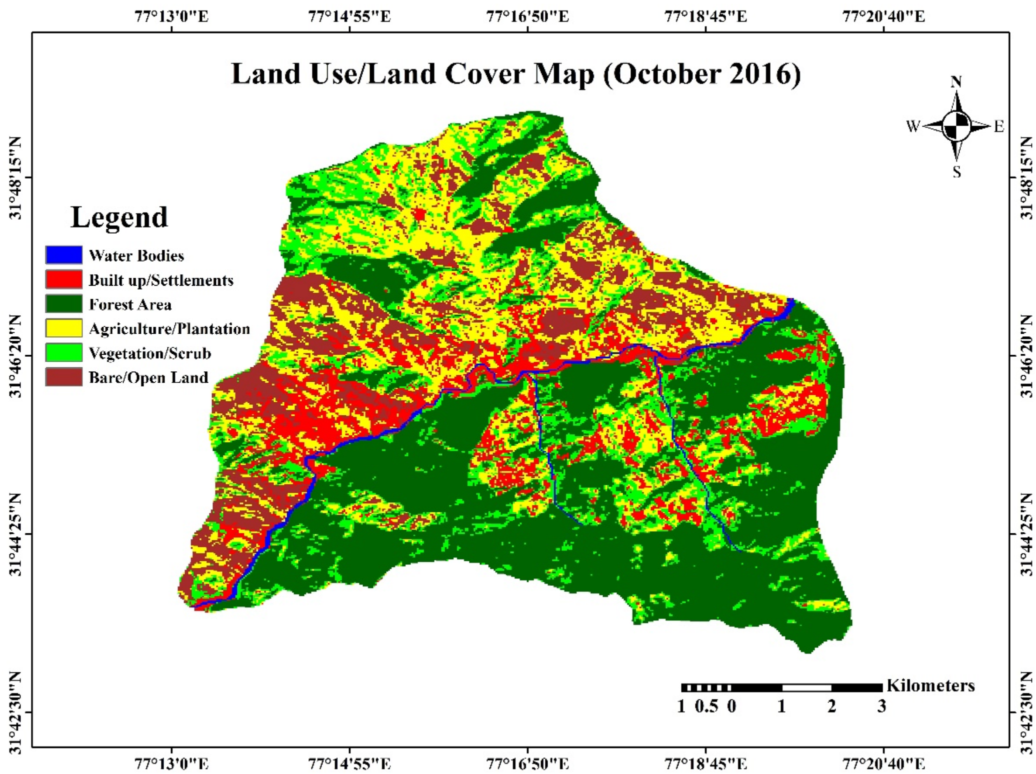

Fig. 3 Land use/land cover of the study area (Year 2016)

Analysis of LST from Landsat 7 (ETM+) and Landsat 8 (OLI) datasets

Landsat 8 TIRS and Landsat 7 (ETM+) data has been utilized for estimating LST of study area. Two types of algorithms were used to estimate LST viz. single channel (SC) equation-based method and split window (SW) algorithm and LST estimation are shown in Fig. 6 and 7 respectively. The land use/land cover (LULC) map (Fig. 2 and 3) was generated for year 2001 and 2016 and has been used in the present study to examine the LST estimates for respective years. The spatial distribution of surface temperature of Landsat 7 (ETM+), for dated 18th October 2001 shows that the LST ranges from minimum 6.15°C to maximum 36.10°C with a mean of 19.98°C and standard deviation of 6.09. The higher LST values corresponds to bare/open land and built-up/settlement of the study area; whereas, lower LST values were observed in forested and agricultural land of the study area (Fig. 2 and 6). The NDVI values also support these LST estimates (Fig. 4).

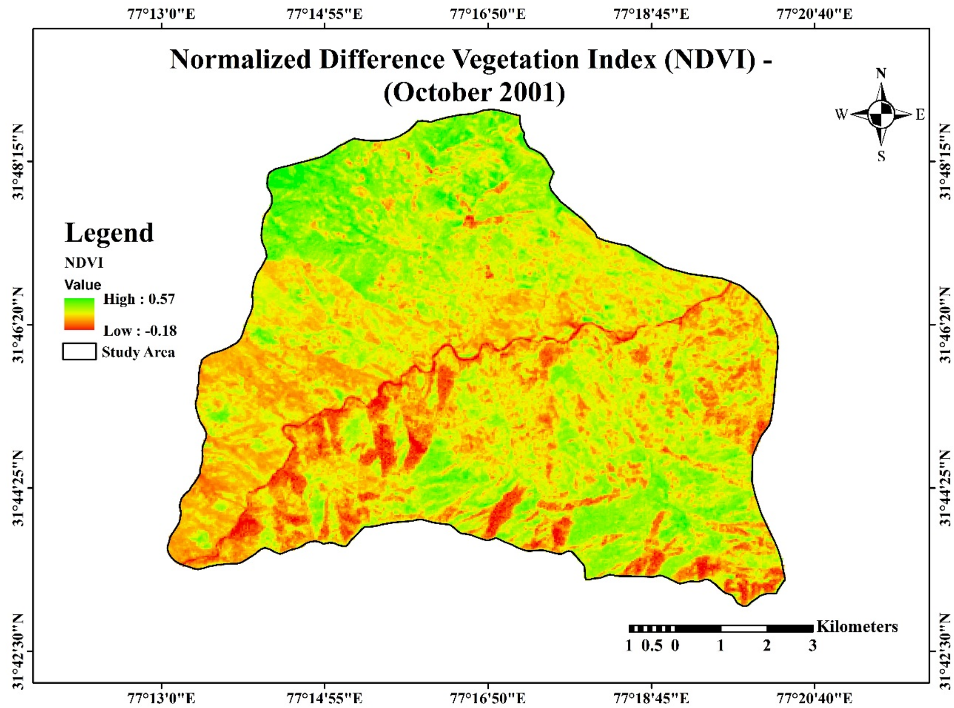

Fig. 4 NDVI derived from Landsat 7 (ETM+) data of October 18, 2001 (Path 147/Row 38)

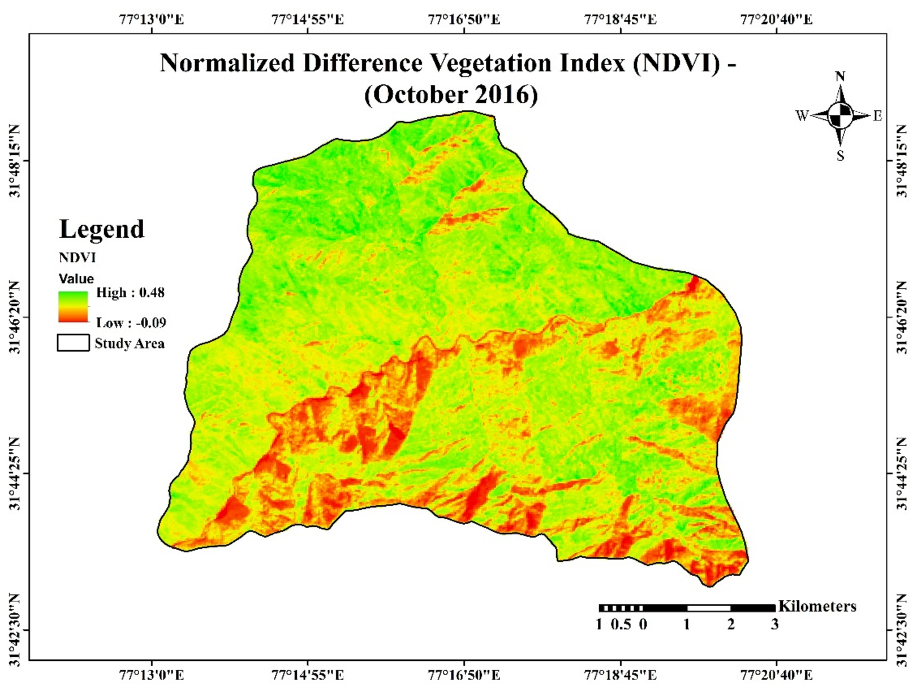

Fig. 5 NDVI derived from Landsat 8 (OLI) data October 19, 2016 (Path 147/Row 38)

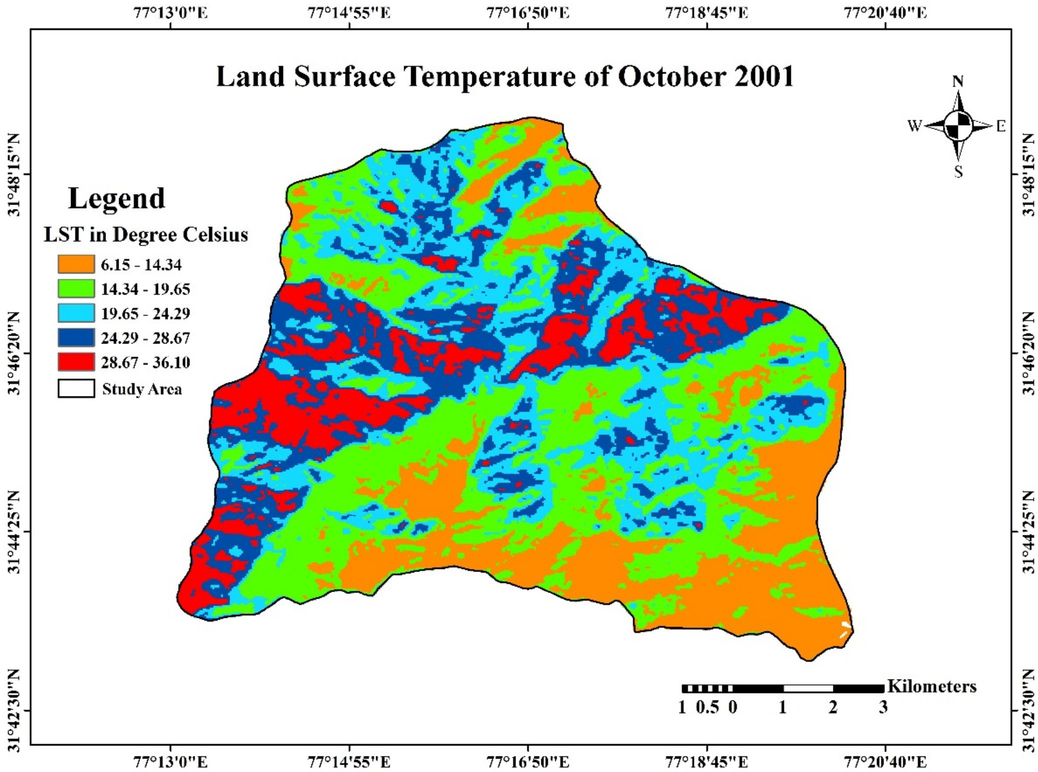

Fig. 6 Spatial distribution of land surface temperature (LST) of Landsat 7 (ETM+) data of 18th October 2001 (Path 147/Row 38)

In the LST products derived using SW algorithm from Landsat 8 for October 2016, the highest value was around 33.31°C, which observed in north and east side which comprise of barren land and settlements area and the areas where development activities are going on; whereas, lower LST value was observed to be 7.16°C in the forested area of the study area (Fig. 3 and 7). The mean LST was observed to be 19.62 °C and standard deviation of 4.95 for October 2016 LST estimates. The highest and lowest values of LST represent the hot and cold spot areas in the study area. It is observed that surface area under the higher LST values is increased from 2001 to 2016. It is noteworthy that, the value of maximum temperature for the year 2016 is lower than that observed in October 2001; but the range of lowest temperature is increased to 7.16°C in 2016 from 6.15°C in 2001 which could be attributed to change in climatic condition in entire Sainj river basin over the period of 15 years. However, detail climate change studies will be required to arrive on conclusion in relation to increasing and decreasing temperature.

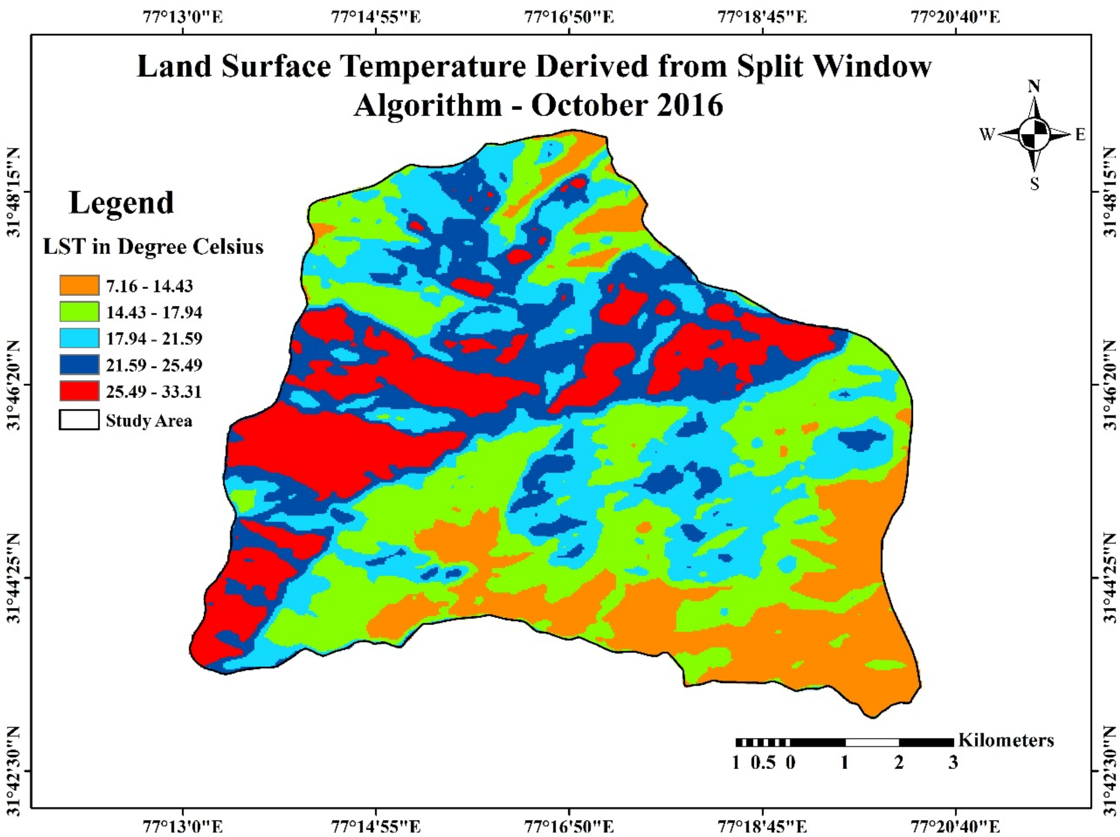

Fig, 7 Spatial distribution of land surface temperature (LST) of Landsat 8 (OLI) data of 19th October, 2016 (Path 147/Row 38)

For validation of LST estimates from Landsat products using single channel and SW algorithm, MODIS LST products of same date and region were used. Further the corresponding land use/land cover change was also analyzed to understand the effect of land use changes on the behavior of land surface temperature. The LST derived from MODIS data products ranges from minimum 16.65°C to maximum 31.85 °C for October 2001 with a mean of 24.41°C and standard deviation 4.43; and minimum 16.14°C to maximum 22.73°C for October 2016 with mean of 19.88°C and standard deviation 1.71 (Fig. 8 and 9). These estimates was not found close to the LST estimate derived from Landsat 7 and 8. The MODIS LST product is of coarser spatial resolution of 1 km compared to LST retrieved using Landsat 7 (ETM+) and Landsat 8(OLI) TIRS data with resolution of 30 m. However, the high temperature zone was found to be same, i.e. barren land/open land and the land with developmental activity and settlement, indicates the reasonable reliability of the retrieved LST. Overall, the hot and cold spots identified in MODIS data products reasonably matches the Landsat LST products.

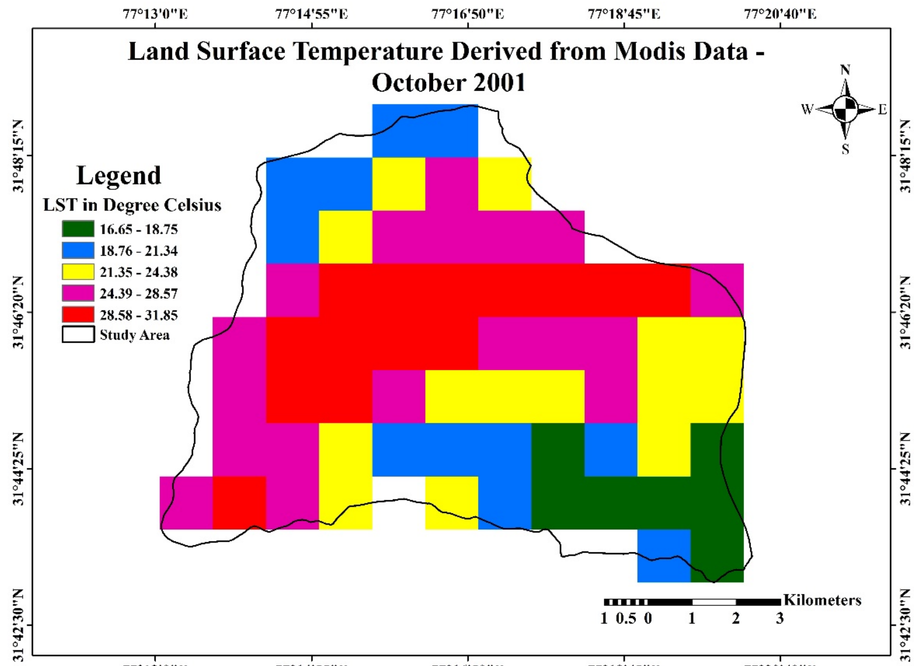

Fig. 8 Spatial distribution of MODIS LST product of 18 October, 2001 (Path 147/Row 38)

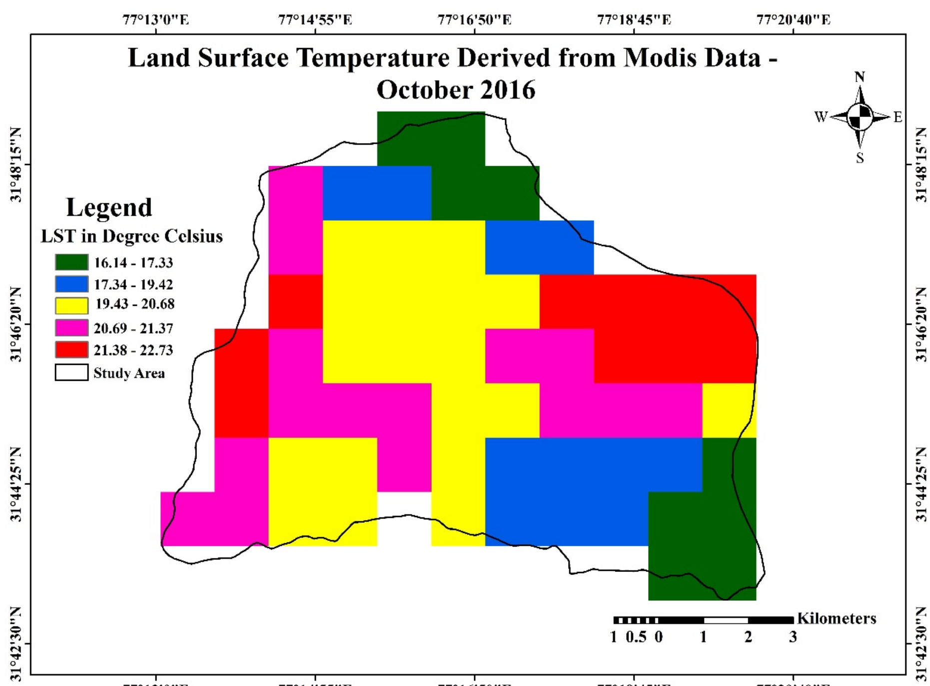

Fig. 9 Spatial distribution of MODIS LST product of 19 October, 2016 (Path 147/Row 38)

This results can be strengthen by correlation and sensitivity analysis for validation purpose and re-sampling technique of MODIS data to avoid problem of coarser resolution on LST estimates.

Conclusion

Present study was conducted in downstream part of Sainj river basin in Himachal Pradesh of Indian Himalayan Region (IHR), wherein we examine the change in LST over different land use/land cover of the area over the period of time (16 years) where developmental activities alters the natural ecosystem in relation to water and land use. LST was derived using Landsat-7 Enhanced Thematic Mapper Plus (ETM+) for October 2001 using Single Channel/Window algorithm and Landsat-8 OLI (Operational Land Imager) for October 2016 using Split-Window (SW) algorithm. NDVI threshold was used for estimating land surface emissivity. The spatial distribution of LST of Landsat 7 of 18th October 2001 was observed in the rages of minimum 6.15°C to maximum 36.10°C with a mean of 19.98°C and standard deviation of 6.09; whereas, for Landsat 8 (OLI), of 22nd October 2016 the LST estimates ranges from minimum 7.16°C to maximum 33.31°C with a mean of 19.62 °C and standard deviation of 4.95. We observed that the estimated LST have tradeoff with the different land use/land cover pattern of the study area and LST represent the hot and cold spot areas in the study area accordingly. The LST estimates of barren/open land, settlement/built-up land was observed to be on higher side and LST estimates of forested cover and agriculture cover was found to on lower side; which shows the accuracy of the LST estimates of Landsat 7 and 8 product using single channel and split window algorithm respectively. The results reveals that the higher vegetative cover such as forested area, agricultural cropland, dense vegetation, sparse vegetation brings down the surface temperature. It is also observed that barren land, and built-up and land developmental activities increases the surface temperature of the area. Increasing surface temperature of study area due to change of natural resources is one of the growing environmental problems. For validation, the standard daily LST product of MODIS has been used for both algorithms. Further the corresponding land use/land cover change was also analyzed to understand the effect of land use changes on the behavior of land surface temperature. The same tradeoff of hot and cold spot was observed in MODIS LST outputs but with comparatively poor estimates of high and low LST values which is attributed to the coarser resolution of MODIS data as compare to Landsat 7 and 8 data. This results can be strengthen by correlation and sensitivity analysis for validation purpose and re-sampling technique of MODIS data to avoid problem of coarser resolution on LST estimates. Further ground based temperature data will add benefit for accuracy of the results. In absence of ground observation of land surface temperature, the relatively accurate estimate of LST from Landsat 7 & 8 satellite images corresponding to different land use/land cover and MODIS data product with suggested improvement can be used for further analysis of natural resource management. This study showed that multi-spectral thermal remote sensing offers great potential for estimating land surface temperature at local and regional scale.

Acknowledgement: The author is thankful to the Director, G. B. Pant National Institute of Himalayan Environment and Sustainable Development, Kosi-Katarmal, Almora, Uttarakhand for providing the facilities in Himachal Regional Centre of the Institute where we could finalize the present work. This work is a small part Spring Rejuvenation Project in Sainj river basin for which we would also like to acknowledge the funding from National Mission on Himalayan Studies (NMHS), MoEFCC, Govt. of India.

Authors Contribution*: Pawan Kumar Thakur (JRF) performing the research work and data collection; Vaibhav E. Gosavi (Scientist) has responsible for performing the guidance the research work and is the main corresponding author of manuscript.*

References

Chakraborty, S. D., Kant, Y., Mitra, D., 2013. Assessment of land surface temperature and heat fluxes over Delhi using remote sensing data, *Journal of Environmental Management*, 148, 143-152

Jimenez-Munoz, J.C., Sobrino, J.A., 2008. Split-window coefficients for land surface temperature retrieval from low-resolution thermal infrared sensors, *IEEE Geoscience and Remote Sensing Letters,* 5(4), 806-809

Kalnay, E., Cai, M., 2003. Impact of urbanization and land-use change on climate, *Nature,* 423(6939), 528-531

Kanga, S., Singh, S. K., Sudhanshu., 2017. Delineation of Urban Built-Up and Change Detection Analysis using Multi-Temporal Satellite Images, *International Journal of Recent Research Aspects*, 4(3), 1-9

Karnieli, A., Agam, N., Pinker, R.T., Anderson, M., Imhoff, M.L., Gutman, G.G., Panov, N., Goldberg, A., 2010. Use of NDVI and land surface temperature for drought assessment: merits and limitations, *Journal of Climate*, 23(3), 618–633

Kustas, W.P., Norman, J.M., 1996. Use of remote sensing for evapotranspiration monitoring over land surfaces, *Hydrological Sciences Journal*, 41(4), 495–516

Li, Z-L., Tang, B., Wu, H., Ren, H., Yan, G., Wan, Z., Trigo, I.F., Sobrino, J.A., 2013a. Satellite-derived land surface temperature: current status and perspectives, *Remote Sensing of Environment*, 131, 14-37

Li, Z-L., Wu, H., Wang, N., Qiu, S., Sobrino, J.A., Wan, Z., Tang, B-H., Yan, G., 2013b. Land surface emissivity retrieval from satellite data. *International Journal of Remote Sensing,* 34(9-10), 3084-3127

Li, Z. L., Becker, F., 1993. Feasibility of land surface temperature and emissivity determination from AVHRR data, *Remote Sensing of Environment*, 43, 67-85

McMillin, L.M., 1975. Estimation of sea surface temperatures from two infrared window measurements with different absorption, *Journal of Geophysical Research*, 80(36), 5113-5117

Nikam, B. R., Ibragimov, F., Chouskey, A., Garg, V., Aggarwal, S. P., 2016. Retrieval of land surface temperature from Landsat 8 TIRS for the command area of Mula irrigation project, *Environmental Earth Sciences*, 75, 1169

Parida, B. R., Oinam, B., Patel, N. R., Sharma, N., Kandwal, R., Hazarika, M. K., 2008. Land surface temperature variation in relation to vegetation types using MODIS satellite data in Gujarat state of India, *International Journal of Remote Sensing*, 29 (14), 4219-4235

Price, J.C., 1984. Land surface temperature measurements from the split window channels of the NOAA 7 Advanced very high resolution radiometer, *Journal of Geophysical Research*, 89(D5), 7231-7237

Qin, Z., Karnieli, A., 1999. Progress in the remote sensing of land surface temperature and ground emissivity using NOAA_AVHRR data, *International Journal of Remote Sensing*, 20, 2367-2393

Ramanathan, V., Crutzen, P., Kiehl, J.,Rosenfeld, D., 2001. Aerosols, Climate and the Hydrological Cycle, *Science,* 294(5549), 2119–2124

Rozenstein, O., Qin, Z., Derimian, Y., Karnieli, A., 2014. Derivation of land surface temperature for Landsat-8 TIRS using a split window algorithm. *Sensors,* 14(4), 5768-5780

Singh, O., Sarangi, A., Sharma, M. C., 2008. Hypsometric integral estimation methods and its relevance on erosion status of north-western lesser Himalayan watersheds, *Water Resource Management*, 22, 1545-1560

Singh, S. K., 2016. Geospatial Technique for Land use/Land cover mapping using Multi-Temporal Satellite Images: A case study of Samastipur District (India), *Environment & We: An International Journal of Science & Technology*, 11 (2-4), 75-85

Skokovic, D., Sobrino, J.A., Jimenez-Munoz, J.C., Soria, G., Julien, Y., Mattar, C., Jordi, C., 2014. *Calibration and validation of land surface temperature for Landsat 8-TIRS sensor*, Presentation given in workshop on land product validation and evolution, ESA/ESRIN, January 28-30, 2014

Wan, Z., Wang, P., Li, X., 2004. Using MODIS land surface temperature and normalized difference vegetation index products for monitoring drought in the southern Great Plains, USA, *International Journal of Remote Sensing*, 25(1), 61-72

Yu, X., Guo, X., Wu, Z., 2014. Land surface temperature retrieval from Landsat 8 TIRS-comparison between radiative transfer equations based method, split window algorithm and single channel method, *Remote Sensing*, 6(10), 9829-9852